

## Performance of ITER as burning plasma experiment

M. Shimada 1), V. Mukhovatov 1), G. Federici 2), Y. Gribov 1), A. Kukushkin 2),  
Y. Murakami 3), A. Polevoi 1), V. Pustovitov 4), S. Sengoku 5), M. Sugihara 1)

1) International Team, ITER Naka JWS, Mukouyama, Naka-machi, Naka-gun, Ibaraki-ken,  
311-0193, Japan,

2) International Team, ITER Garching JWS,

3) Toshiba Corp., Minato-ku, Tokyo

4) Kurchatov Institute, Moscow, Russia

5) Japan Atomic Energy Research Institute, Naka-machi, Ibaraki-ken, Japan

e-mail contact of main author : shimadm@itergps.naka.jaeri.go.jp

**Abstract.** Recent performance analysis has improved confidence in achieving  $Q \geq 10$  in inductive operation in ITER. Performance analysis based on empirical scaling shows the feasibility of achieving  $Q \geq 10$  in inductive operation, particularly with improved modeling of helium exhaust. Analysis has also elucidated a possibility that ITER can potentially demonstrate  $Q$ 's  $\sim 50$ , enabling studies of self-heated plasmas. Theory-based core modeling indicates the need of high pedestal temperature (2.3 - 4.5 keV) to achieve  $Q \geq 10$ , which is in the range of projection with presently available pedestal scalings. Pellet injection from high-field side would be useful in enhancing  $Q$  and reducing ELM heat load in high plasma current operation. If the ELM heat load is not acceptable, it could be made tolerable by further tilting the target plate. Steady state operation scenarios at  $Q = 5$  have been developed with modest requirement on confinement improvement and beta ( $H_{98(y,2)} \geq 1.3$  and  $\beta_N \geq 2.6$ ). Stabilisation of RWM, required in such regimes, is feasible with the present saddle coils and power supplies with double-wall structure taken into account. Recent analysis shows a potential of high power steady state operation with a fusion power of 0.7 GW at  $Q \sim 8$ . Achievement of the required  $\beta_N \sim 3.6$  by RWM stabilisation is a challenge and further analysis is also needed on the reduction of the divertor target heat load.

### 1. Introduction

Analysis of ITER plasma performance is being carried out to confirm the integrity of core, pedestal and divertor characteristics. The core performance analysis described in Final Design Report of ITER [1] was based on empirical scaling. Recently efforts have been focused on projection with theory-based modeling in the core. The pedestal temperature has been found to play an important role in core confinement. Improved assessment of the erosion of the target has led to an increase in the tolerable ELM heat load by a factor of  $\sim 2$ . The ELM amplitudes show reduction toward high edge collisionality and high frequency, suggesting that pellet-induced or spontaneous frequent ELMs can suppress the ELM amplitudes to a benign level in ITER. Steady state operation scenarios, with less demanding confinement improvement and beta, have been developed, and analysis of RWM suggests that the present set-up of pick-up coils, vacuum vessel and coils is adequate for RWM stabilisation. Recently scenarios have been developed for high power steady state operation, in the prospect of developing a core plasma for the next step. This paper summarises recent progress in these areas for ITER projection.

### 2. Inductive operation

Performance analysis based on empirical scaling demonstrates the feasibility of achieving its mission of  $Q \geq 10$  in inductive operation [1,2]. Divertor transport calculations by the B2/Eirene code indicate that the steady-state target heat load can be reduced to  $< 10$  MW/m<sup>2</sup> and the helium concentration to  $< 3\%$  at the separatrix [3], which corresponds to  $< 4.3\%$  at the axis. Inclusion of helium elastic scattering in the divertor plasma further enhances the

helium exhaust efficiency by a factor of  $\sim 3$  [4], which increases  $Q$ , e.g. from 10 to 14. Figure 1 shows  $Q$  vs.  $H_{H98(y,2)}$  at a condition that the separatrix power higher than LH transition power  $P_{sep} \geq P_{L-H}$  at a plasma current of 15 MA with different levels of helium concentration [2], suggesting the potential of operating at  $Q$ 's higher than 50 for the investigation of self-heated plasmas.

Core performance projection is also in progress with theory-based modeling e.g. Weiland [5], Multi-Mode [6] and GLF23 [7] models. Figure 2 shows  $Q$  vs. pedestal ion temperature ( $T_{ped}$ ) calculated with Weiland and MMM95 models, showing that the goal of  $Q \geq 10$  is achievable with  $T_{ped} \geq (2.3 - 3.9)$  keV, while the IFS/PPPL model requires  $T_{ped} \geq 4.5$  keV [2]. Analysis of the international pedestal database suggests that achievement of this high pedestal temperature is possible [2,6,8,9,10]. Figure 3 shows a scaling of pedestal pressure compared against experimental data in International Pedestal Database v. 3. This scaling projects a temperature of 5.3 keV for a pedestal density of  $7 \times 10^{19} \text{ m}^{-3}$  [11], suggesting that  $Q \geq 10$  is achievable.  $Q \geq 10$  operation at a plasma current of 15 MA is associated with  $\beta_N \geq 1.5$ , which could trigger neoclassical tearing modes (NTMs). Present analysis suggests that stabilisation of full-grown 2/1 and 3/2 of NTM could require electron cyclotron current drive (ECCD) power of  $\sim 30$  MW [12]. An early detection of the island with a size  $w/a \sim 0.04$  and subsequent ECW injection could enable mode stabilisation within the initial capability of the ECCD/ECH system (20 MW) [13].

### 3. ELM

The projection of the heat load with type-I ELMs in the inductive high  $Q$  operation is subject to a large uncertainty. However, recent calculations show that with a reasonable rise time (0.3 ms) of target heat load and a reasonable heat conductivity taken into account, the tolerable target heat load is  $\sim 1 \text{ MJ/m}^2$  [14] or  $\sim 6 \text{ MJ}$  per ELM pulse with a total ELM footprint of  $6 \text{ m}^2$ , which corresponds to about 6 % of the pedestal energy. The projected ELM heat load is 5 - 20 MJ in ITER [14]. As will be discussed in the following section, pellet injection could reduce the ELM amplitudes to a benign level. If the heat load is excessive, further inclination of the target would increase the heat load that can be tolerated. Furthermore, extension of the lifetime of the target plates is possible, e.g. operation with more benign type-II ELMs with a small decrease of plasma current [15]. Therefore in steady-state operation and long pulse hybrid operation with a reduced plasma current, a long lifetime is expected.

### 4. Pellet injection

High-field side pellet injection has proved to be successful in maintaining good confinement at densities close to the Greenwald density ( $n_G$ ) [16,17]. Reduction of ELM heat load is also observed [18, 19]. This fuelling method will be one of the major fuelling methods in ITER and is expected to enhance the  $Q$  value and reduce the ELM heat load [20]. Projected fusion power  $> 450 \text{ MW}$ , at an auxiliary heating power of 23 MW and  $Q$  of  $\sim 20$  can be achieved at line-averaged density below the Greenwald density with pellet injection from the high field side at a moderate pellet speed of  $\sim 500 \text{ m/s}$ . The ELM heat loss is observed to decrease to 4-5 % of the pedestal energy with increasing pedestal collisionality in the high density range [21]. Experiments in ASDEX-Upgrade show that the energy loss during pellet-induced ELM is reduced with ELM frequency following the same scaling as spontaneous ELM obtained in JET and ASDEX-Upgrade experiments [19]. Thus pellet injection would increase the collisionality of the pedestal and it is expected to reduce the heat load below a tolerable range in ITER [20]. Calculation shows that the increase in ELM frequency from  $\sim 1 \text{ Hz}$  (without

pellets) to 4 Hz (with pellets) reduces the ELM energy loss from 10 – 20 MJ to below 6 MJ (Fig. 4). The recovery of the pedestal temperature is much faster than the pellet interval, suggesting that the core confinement remains high after the pellet. However, more work is needed to optimise the pellet parameters and to confirm the compatibility of the pellet injection with good confinement and low ELM heat load.

## 5. Steady state operation

Operational scenarios have been developed for steady-state operation with modest requirements on confinement and  $\beta$ ; e.g.  $H_{98(y,2)} \geq 1.3$ ,  $\beta_N \geq 2.6$  [22], with  $I_p = 9$  MA,  $Q = 5$ ,  $n/n_G = 0.83$ ,  $Z_{\text{eff}} = 2.2$  and  $P_{\text{aux}} = 68$  MW. The plasma parameters are shown in Table 1. Divertor transport calculations by the B2/Eirene code show that long connection length with steady-state operation at higher safety factor facilitates divertor compatibility even with a higher fusion power [3]. As the required  $\beta_N$  exceeds the ideal MHD no-wall limit for these scenarios by 10-20 %, suppression of resistive wall modes (RWMs) will become a key issue.

Stability against ideal modes has been analysed for three sets of safety factor and pressure profiles shown in Fig. 5 (a) with the KINX code [22]. The minimum  $q$  of these reverse shear equilibria are 2.1, 2.25 and 2.4. As neoclassical heat and particle diffusivities are assumed inside the minimum- $q$  radius, the pressure profile becomes flatter with higher minimum  $q$ . The most dangerous mode is an external  $n = 1$  kink mode coupled to internal modes. The stabilising ideal wall position  $a_w/a$  is shown against normalised  $\beta$  in Fig. 5 (b). The no-wall limit increases with flatter pressure profiles with higher minimum  $q$ . The ideal wall radius  $a_w$  for marginal stability increases significantly with a flatter pressure profile at higher minimum  $q$ . The effective wall position  $a_w/a$  is 1.375 for the plasma shown in Table 1, shifted outward by 0.15 m with a reduced minor radius ( $a = 1.85$  m). At this wall position, the marginal  $\beta_N$  is 2.6 for a minimum  $q$  of 2.1 and 3.6 for a minimum  $q$  of 2.4. A full-bore plasma with  $R = 6.2$  m and  $a = 2$  m is more stable against ideal modes with  $a_w/a = 1.345$ , suggesting that high  $\beta_N \sim 3.6$  steady state operation with  $Q \sim 10$ , described in the following section, could be made stable with an ideal wall.

Analytical study has been carried out with double-wall structure of the ITER resistive vacuum vessel taken into account. The double wall structure does not affect the RWM growth rate significantly, but deteriorates the feedback stabilisation. However, the present arrangement of saddle coils and power supply is adequate for RWM stabilisation for the range of  $\beta_N$  anticipated for the steady state operation scenarios quoted above [23, 24].

## 6. High performance steady state operation

Recently high power steady state operation has attracted much interest from the viewpoint of developing a core plasma of a fusion power plant, in which the requirement is more demanding on  $\beta$ ,  $Q$ , power and particle control and bootstrap current fraction. Figure 6 shows profiles of current density, safety factor, temperature and electron density calculated with the ASTRA code for possible ITER conditions. A combination of neutral beam current drive at the core, lower hybrid current drive at  $r/a \sim 0.7$  and bootstrap current provides a 12 MA weak-reverse-shear (WRS) steady state plasma, with a  $q_{\text{min}}$  at  $r/a \sim 0.7$ .  $q_{95} = 4.76$ ,  $H_{98(y,2)} = 1.53$ , and fraction of Greenwald density  $n_e/n_G = 0.86$ . The bootstrap current fraction is 54.5 %. The fusion power is 700 MW and the current drive power is 47 MW (NB) and 40 MW (LH), giving a  $Q$  value of 8. Neoclassical heat and particle diffusivities are assumed inside the radius of minimum  $q$ . A burn phase of  $\sim 300$  s can be sustained with the present ITER

hardware, which is adequate to reach a quasi-steady state with an optimised start-up scenario. The value of  $\beta_N$  in this discharge is 3.6, which is above the no-wall limit of 2.8 and below the ideal wall limit of 3.8. Requirement on RWM stabilisation is being analysed.

In addition to beta, the divertor heat load and helium exhaust are also of major concern in high power operation. The divertor performance was estimated with a scaling [25] derived from a series of B2-Eirene runs at  $q_{95} = 3$ . Since this discharge has a higher safety factor ( $q_{95} = 4.76$ ), this estimate provides a conservative value. Figure 7 shows peak target heat load, separatrix electron density, helium concentration at the separatrix, and DT throughput with a scrape-off layer power of 155 MW and a pumping speed of  $10 \text{ m}^3/\text{s}$  for the discharge shown in Fig. 6. With an increase in DT throughput, the helium concentration and peak heat load are reduced substantially, reaching 0.35 % and  $< 5 \text{ MW/m}^2$ , respectively at a DT throughput of  $200 \text{ Pa m}^3/\text{s}$ . Although the helium density at the separatrix is maintained at a very low level, further analysis is needed on helium transport with the internal transport barrier.

A high fusion power ( $\sim 1 \text{ GW}$ ) plasma condition, i.e. high  $\beta_N$  and high power exhaust, can be simulated with a plasma with an isotopic fraction of  $\sim 0.2$  or  $0.8$  at an acceptable fusion power in ITER, i.e. 700 MW. The reduced alpha heating power can be compensated for by increased additional power, as shown in Fig. 8. To maintain the fusion power below 700 MW and additional power below 115 MW, the operation point should fall into either one of the two shaded regions in the figure. The plasma current of 15 MA,  $\beta_N = 3.0$ ,  $\langle n_e \rangle / n_G = 0.9$ ,  $n_{e0} / \langle n_e \rangle = 1.3$ , and  $H_{H98(y,2)} = 1.3$  are assumed. The expected bootstrap current is 33 % and the total non-inductively driven current is 57 %. This operation can be sustained for  $\sim 300 \text{ s}$ .

## 7. Conclusions

- 1) Performance analysis based on empirical scaling demonstrates the feasibility of achieving  $Q \geq 10$  in inductive operation, especially with improved model of helium exhaust.
- 2) Theory-based core modeling indicates the need of high pedestal temperatures (2.3 - 4.5 keV) to achieve  $Q \geq 10$ , which is in the range of projection with presently available pedestal scalings.
- 3) The heat load of type-I ELM in high plasma current operation could be made tolerable by high density operation and further tilting the target plate (if necessary).
- 4) Pellet injection from the high-field side would be useful in enhancing  $Q$  and reducing ELM heat load.
- 5) Steady state operation scenarios to achieve  $Q = 5$  have been developed with modest requirement on confinement improvement and beta ( $H_{H98(y,2)} \geq 1.3$  and  $\beta_N \geq 2.6$ ). Stabilisation of RWM, required in such regimes, is feasible with the present saddle coils and power supplies with double-wall structure taken into account.
- 6) Recent analysis shows a possibility of high power steady state operation with a fusion power of e.g. 0.7 GW at  $Q \sim 8$ . Achievement of the required  $\beta_N \sim 3.6$ , above the no-wall limit (2.8) and below ideal wall limit (3.8), by RWM stabilisation is a challenge and further analysis is also needed on the reduction of the divertor target heat load.
- 7) With an isotopic mixture of  $\sim 0.2$  or  $\sim 0.8$ , there is a possibility of simulating a plasma

condition with a fusion power of 1 GW, e.g. high  $\beta$  and power and particle control within the capability of the ITER hardware.

#### Reference

- [1] ITER Technical Basis, ITER EDA Documentation Series No. 24, IAEA, Vienna, 2002.  
 [2] MUKHOVATOV, V., et al., this Conference, CT/P-03.  
 [3] KUKUSHKIN, A. 28<sup>th</sup> EPS Conf. on Contr. Fusion and Plasma Phys., Funchal, 18-22 June 2001, P5105, ECA, Vol. 25A (2001) 2113.  
 [4] KUKUSHKIN, A., et al., Plasma Physics and Controlled Fusion 44 (2002) 931.  
 [5] WEILAND, J., 28<sup>th</sup> EPS Conf. On Contr. Fusion and Plasma Phys., Funchal, 18-22 June 2001, P2039, ECA, Vol. 25A (2001) 633.  
 [6] BATEMAN, G., Kritz, A.H., Onjun, T. and Pankin, A., private communication (2002).  
 [7] KINSEY et al., private communication (March, 2002).  
 [8] SUGIHARA, M., et al., Nucl. Fusion 40 (2000) 1743.  
 [9] THOMSEN, K., Cordey, J.G., et al., to be published in Plasma Phys. and Contr. Fusion.  
 [10] CORDEY, et al., ITPA Meeting, 11-14 March 2002, PPPL, Princeton, NJ, U.S.A.  
 [11] SUGIHARA, M. et al., to be published.  
 [12] GIRUZZI, G., ITPA Meeting on MHD, Disruption and Control, Feb. 2002.  
 [13] ZVONKOV, A., ITPA Meeting on MHD, Disruption and Control, Feb. 2002.  
 [14] FEDERICI, G., et al., PSI Conference (2002), to be published in J. Nucl. Mat.  
 [15] KAMADA, Y., Plasma Physics and Controlled Fusion 42 (2000) A247.  
 [16] LANG, P.T., et al., Nucl. Fusion 40 (2000) 245.  
 [17] LANG, P.T., et al., 28<sup>th</sup> EPS Conf. on Contr. Fusion and Plasma Phys., Funchal, 18-22 June 2001, ECA, Vol. 25A (2001) 973.  
 [18] LOARTE, A., et al., 28<sup>th</sup> EPS Conf. on Contr. Fusion and Plasma Phys., Funchal, 18-22 June 2001, ECA, Vol. 25A (2001) 945.  
 [19] LANG, P.T., et al., 29<sup>th</sup> EPS Conf. on Contr. Fusion and Plasma Phys., Montreux, 17-21 June 2001, ECA, Vol. 26A (2002) P1-004.  
 [20] POLEVOI, A., et al., this Conference, CT/P-09.  
 [21] LOARTE, A., IAEA-CN-77/ITERP/11, 18th IAEA Fusion Energy Conference (2000).  
 [22] POLEVOI, A., et al., this Conference, CT/P-08.  
 [23] GRIBOV, Y., et al., this Conference, CT/P-12.  
 [24] LIU, Y., BONDESON, A., GREGORATTO, D., this Conference, TH/P3-12.  
 [25] PACHER, H., et al., PSI Conference (2002), to be published in J. Nucl. Mat.

**Table 1.** ITER plasma parameters for the steady state scenario

Parameter	Value	Parameter	Value
R/a, m	6.35 /1.85	$\langle T_e \rangle_n / \langle T_i \rangle_n$ , keV	11/12-10.5/11
$\delta_{95}/\kappa_{95}$	0.41/1.84	$W_{th}/W_{fast}$ , MJ	273/60-255/50
$q_{95}$	5.16-5.13	$H_{H98(y,2)}$	1.41-1.3
$I_p$ , MA/ $\langle n_e \rangle, 10^{19} m^{-3}$	9 /6.74	Q	5.7-5
$\beta_N$	2.8-2.56	$P_{NB}/P_{LH}$ , MW	34/29-33.7
$l_i$	0.72-0.63	$P_{fus}/P_s$ , MW	361/93-338/97
$\langle Z_{eff} \rangle$	2.2-2.17	$\tau_E$ , s	2.54-2.32

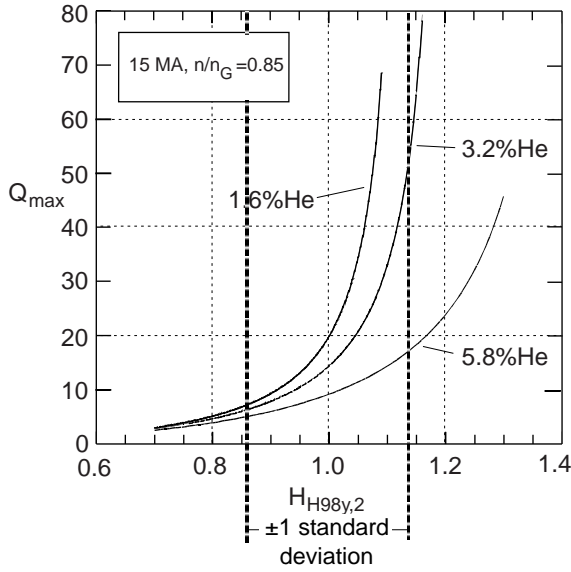
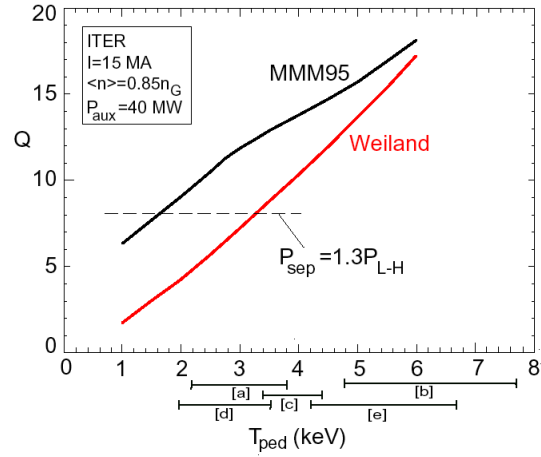


FIG. 1.  $Q_{max} = P_{fusion}/P_{add}$  ( $P_{loss} = P_{L-H}$ ) vs.  $H_{H98(y,2)}$  with different levels of helium at a plasma current of 15 MA, showing that significant improvement of performance is expected with improved helium modeling, and that  $Q > 50$  is a possibility.



[a] MHD limit pedestal model, J.G.CORDEY, et.al, this Conference, CT/R-02  
 [b] Thermal conduction pedestal model, J.G.CORDEY, et.al, this Conference, CT/R-02  
 [c] MHD limit pedestal model, M.SUGIHARA, et al., Nucl. Fusion **40** (2000) 1743  
 [d] MHD limit pedestal model, A.KRITZ, et al. EPS -29 (Montreux, 2002) D-5.001  
 [e] MHD limit pedestal model, M.SUGIHARA, et al., 57th Annual Meeting of Phys. Soc. Japan (2002).

FIG. 2.  $Q$  versus  $T_{ped}$  predicted for ITER by the Multi-Mode and Weiland models. Dashed line show a value of  $Q$  compatible with  $P_{sep} = 1.3 \times P_{L-H}$ , and horizontal bars show the ranges of  $T_{ped}$  predicted for ITER by different pedestal scalings.

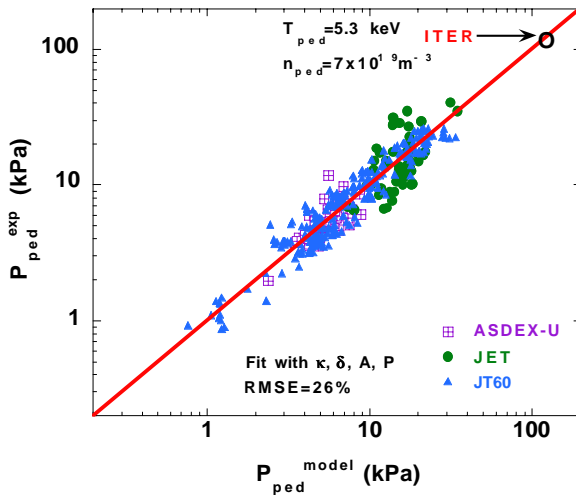


FIG. 3. Scaling of Pedestal pressure compared against experimental data in International Pedestal Database. This scaling projects a pedestal temperature of 5.3 keV for a pedestal density of  $7 \times 10^{19} \text{ m}^{-3}$  in ITER.

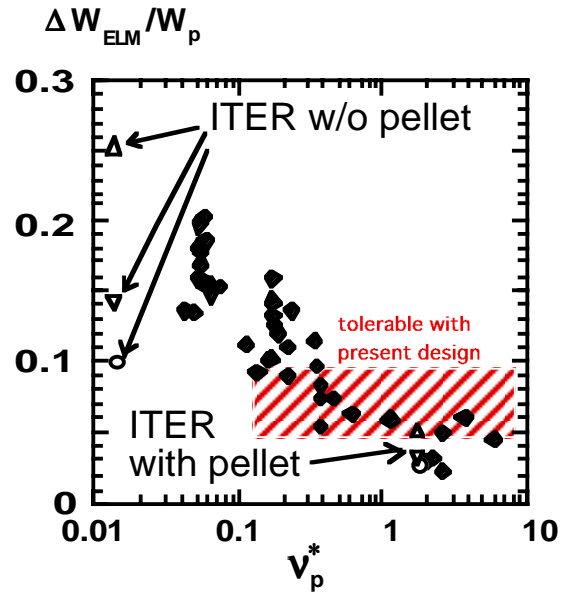


FIG. 4. Dependence of fraction of pedestal energy loss  $\Delta W_{ELM}/W_p$  on the pedestal collisionality  $v_p^*$ . Experimental points [20] are shown by closed diamonds together with predictions for ITER (open points) with and without pellet.

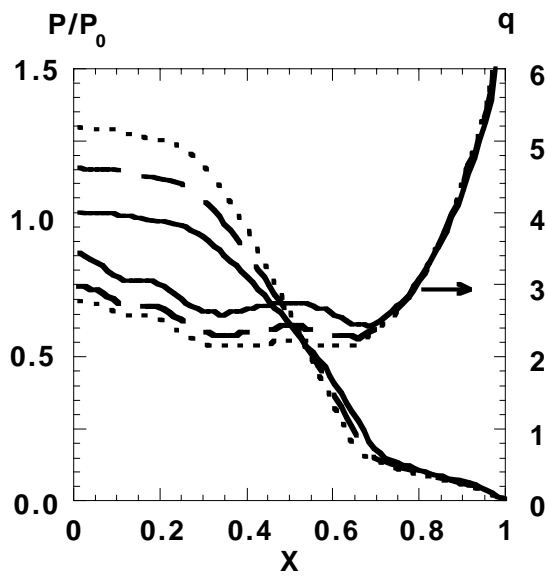


FIG. 5 (a). Three different  $q$  profiles for ideal kink mode calculation of weak reverse shear configuration for steady state operation. The minimum  $q$ 's are 2.1(dotted), 2.26(dashed) and 2.4(solid). Plasma pressure profiles are also shown, which are calculated with neoclassical heat and particle diffusivities inside the minimum- $q$  radius.

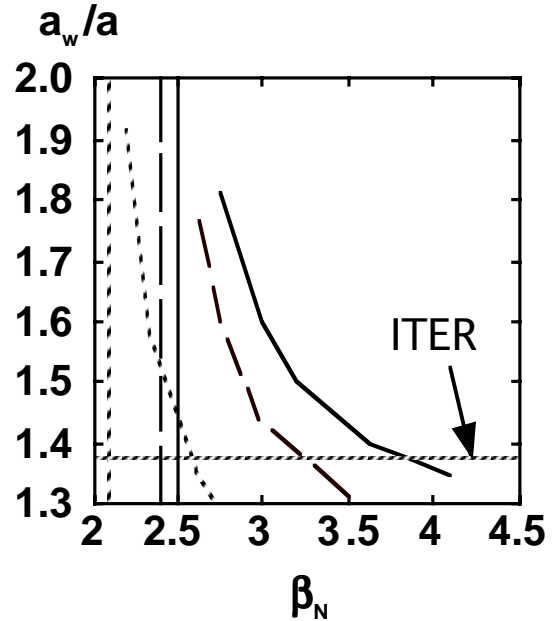


FIG. 5 (b). Stabilising wall position  $a_w/a$  vs. normalised beta  $\beta_N$  for  $q=\text{const}$  scan of SS operational points shown in FIG. 5 (a), and  $a = 1.85$  m. The no-wall limits are shown by vertical lines. The  $a_w/a$  of a reduced-size plasma of ITER shifted 0.15 m outward is indicated with a horizontal dotted line.

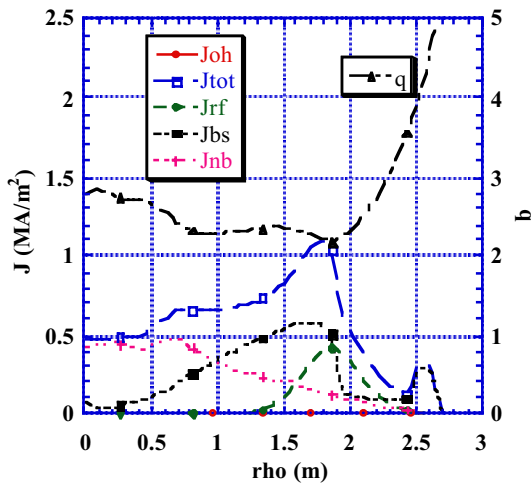


FIG. 6 (a). Radial profiles of current density and safety factor for a steady state discharge with 700 MW fusion power. Combination of neutral current drive at the core, RF current drive at 70% of minor radius and bootstrap current results in weak reverse shear.

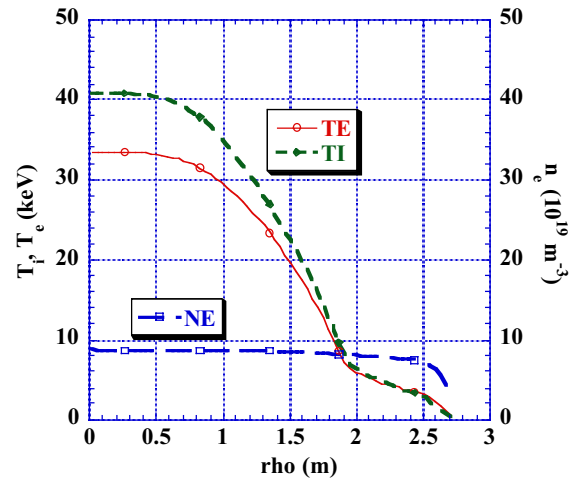


FIG. 6 (b). Radial profiles of ion and electron temperature and electron density for the discharge in FIG. 6(a). Neoclassical heat and particle diffusivities are assumed inside the radius of minimum  $q$ .

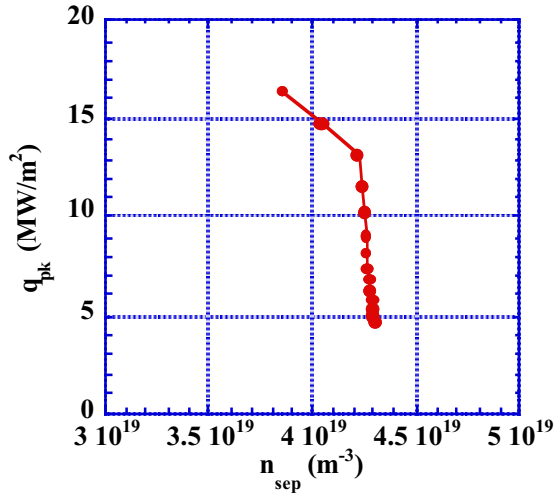


FIG. 7 (a). Peak target heat load against separatrix density for the condition of high power steady state discharge shown in FIG. 6. Increased particle throughput results in increase in separatrix density and decrease in peak target heat load.

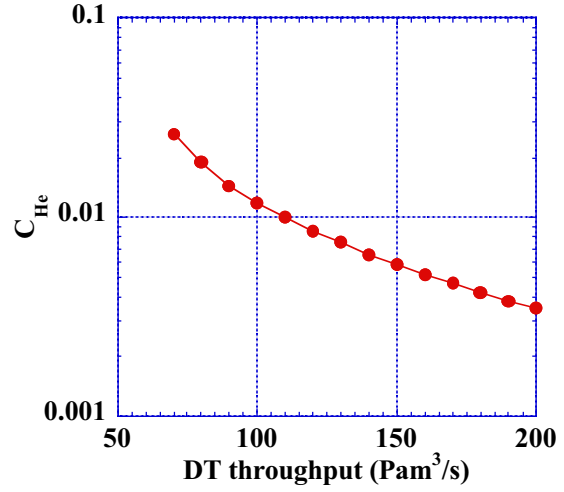


FIG. 7 (b). Helium concentration at the separatrix against particle throughput of high power steady state discharge shown in FIG. 6.

$I_p = 15$  MA,  $\beta_N = 3.0$ ,  $\langle n_e \rangle / n_G = 0.9$ ,  $n_{e0} / \langle n_e \rangle = 1.3$ ,  $H_{H98(y,2)} = 1.3$

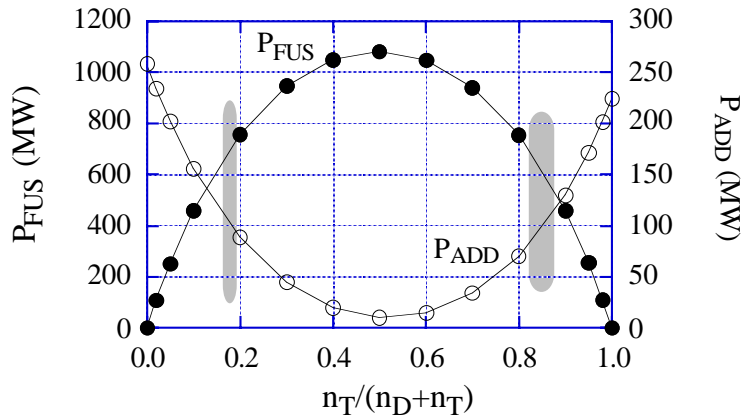


FIG. 8. Fusion power against DT isotope ratio. Reduction of alpha-heating power can be compensated for by increase in additional power. The operation point should be in either one of the two shaded zones, where the fusion power is within the hardware limit, i.e. 700 MW, and the required additional power is within the power available, i.e. 115 MW.